Framework for Probabilistic Projections of Energy-Relevant Streamflow Indicators under Climate Change Scenarios for the U.S.

Final Technical Report

U.S. Department of Energy

DE-FG02-08ER64641

Thorsten Wagener (PI)
Department of Civil Engineering, University of Bristol, Bristol U.K.

Michael Mann (Co-PI)
Department of Meteorology, The Pennsylvania State University, University Park, PA 16802, USA

Robert Crane (Co-PI)
Department of Meteorology, The Pennsylvania State University, University Park, PA 16802, USA

April 2014

Executive Summary

This project focuses on uncertainty in streamflow forecasting under climate change conditions. The objective is to develop easy to use methodologies that can be applied across a range of river basins to estimate changes in water availability for realistic projections of climate change. There are three major components to the project:

1) Empirical downscaling of regional climate change projections from a range of Global Climate Models
2) Developing a methodology to use present day information on the climate controls on the parameterizations in streamflow models to adjust the parameterizations under future climate conditions (a trading-space-for-time approach)
3) Demonstrating a bottom-up approach to establishing streamflow vulnerabilities to climate change.

The results reinforce the need for downscaling of climate data for regional applications, and further demonstrates the challenges of using raw GCM data to make local projections. In addition, it reinforces the need to make projections across a range of global climate models. The project demonstrates the potential for improving streamflow forecasts by using model parameters that are adjusted for future climate conditions, but suggests that even with improved streamflow models and reduced climate uncertainty through the use of downscaled data, there is still large uncertainty is the streamflow projections.

The most useful output from the project is the bottom-up vulnerability driven approach to examining possible climate and land use change impacts on streamflow. Here, we demonstrate an inexpensive and easy to apply methodology that uses Classification and Regression Trees (CART) to define the climate and environmental parameters space that can produce vulnerabilities in the system, and then feeds in the downscaled projections to determine the probability top transitioning to a vulnerable sate. Vulnerabilities, in this case, are defined by the end user.

1. Goals, Objectives and Accomplishments

The primary goals of the project were to:

1) Downscale Global Climate Model (GCM) data to produce regional scale climate change projections for the Susquehanna River Basin.
2) Use the downscaled climate data to drive a river basin model to assess potential changes in river flow under likely climate change conditions.
3) Develop a methodology that could be easily applied to other river basins across the country.

The first goal was accomplished and resulted in two publications:

Ning, L., M. E. Mann, R. G. Crane, T. Wagener, R. Najjar, R. Singh. Probabilistic Projections of Anthropogenic Climate Impacts on Precipitation for the Mid-Atlantic Region of the United States. **J. Climate**, 25:5273-5291 (2012).

Ning, L., M. E. Mann, R. G. Crane, T. Wagener. Probabilistic Projections of Climate Change for the Mid-Atlantic Region of the United States—Validation of Precipitation Downscaling During the Historical Era. **J. Climate**, 25:509-526 (2012).

Developing a watershed model to address the second goal highlighted significant issues with cascading uncertainty through the model hierarchy from the GCMs down to the river basin model. This led to an alternative approach to predict streamflow under a changing climate utilizing a trading-space-for-time approach to probabilistic continuous streamflow predictions, described in:

Singh,R., K. van Werkhoven, T. Wagener. Hydrological impacts of climate change in gauged and ungauged watersheds of the Olifants basin: a trading-space-for-time approach**, Hydrological Sciences Journal**, 59:1, 29-55, DOI: 10.1080/02626667.2013.819431 (2014)

Singh, R., T. Wagener, K. van Werkhoven, M. E. Mann, and R. Crane. A trading-space-for-time approach to probabilistic continuous streamflow predictions in a changing climate – accounting for changing watershed behavior. **Hydrol. Earth Syst. Sci**., 15:3591–3603 (2011).

Possibly the most significant accomplishment in terms of assessing water supply potential under changing climate conditions, and in terms of developing an easily adaptable model for other locations (goal 3) was the development of a bottom-up approach that allows water managers to identify critical hydrologic indicator thresholds and to then to assess their vulnerability to climate or other environmental changes. This approach is described in:

Singh, R., T. Wagener, R. Crane, M.E. Mann, L. Ning. A vulnerability driven approach to identify adverse climate and land use change combinations for critical hydrologic indicator thresholds—Application to a watershed in Pennsylvania, USA**. Water Resources Research**, DOI: 10.1002/2013WR014988 (2014)

2. Project Activities

2.1 Regional Climate Downscaling

The study employed an empirical downscaling methodology developed by Hewitson and Crane (2006) to estimate local precipitation changes from Global Climate model projections. This approach uses Self-Organizing Maps (SOMs) to characterize the large scale state of the atmosphere on a daily basis. We take 17 reporting stations in Pennsylvania and, for each one, establish a 19 element hexagonal grid, centered on the station. The grid has a nominal 2° resolution and we remap the National Center for Climate Prediction (NCEP) 2.5° x 2.5° reanalysis data to the local grid for each station. Data used are *u* and *v* winds at 10m and 700 hPa, specific and relative humidity at 850 hPa, the temperature anomaly at 10m and the lapse rate from 850 to 500 hPa. These data are used to produce a separate 11x9 SOM for each reporting station. In this application, the SOM can be regarded as a non-linear fuzzy clustering algorithm that assigns every day in the NCEP data set to one of the 11x9 SOM nodes (for the period 1979-2007). For each station, we map each day to its SOM node and then take each day's observed precipitation and bin it according to the SOM mapping. For each station and SOM node we can then construct a cumulative probability distribution of the observed precipitation. For the downscaling, we simply map the present day (1961-2000) and future (2046-2065) GCM data to the SOMs and for each station and day, randomly select a precipitation value form the frequency distribution for that node.

We used nine GCMs from the Coupled Climate Intercomparison Project phase 3 (CMIP3) archive for the twentieth century climate with the 20c3m historical greenhouse gas concentrations, and the same nine models for the mid-21st century simulations using the A2 emissions scenario. The models used are the Canadian Centre for Climate Modelling and Analysis (CCCma) Coupled General Circulation Model, version 3.1 (CGCM3.1); Centre National de Recherches Météorologiques Coupled Global Climate Model, version 3 (CNRM-CM3); Commonwealth Scientific and Industrial Research Organisation, Mark 3.0 (CSIRO Mk3.0); Geophysical Fluid Dynamics Laboratory Climate Model, version 2.0 (GFDL CM2.0); Goddard Institute for Space StudiesModel E-R (GISSER); L'Institut Pierre-Simon Laplace Coupled Model, version 4 (IPSL CM4); Meteorological Institute of the University of Bonn, ECHO-G Model (MIUBECHOG); Max Planck Institute (MPI) ECHAM5; and Meteorological Research Institute Coupled General Circulation Model, version 2.3.2a (MRI CGCM2.3.2a). The data and descriptions of the GCMs can be found at the WCRP CMIP3 Multi-Model Data Web site (https://esg.llnl.gov:8443/index.jsp). These nine models were chosen because they archived the variables needed for the SOM mapping at a daily resolution.

The downscaling was very effective at capturing the present day precipitation at each of the stations. Figure 1 shows the probability distributions of observed (black) and downscaled (gray) daily precipitation over the 17 stations during the period 1079-2005. Overall, the downscaling was shown to be effective at capturing the daily variability in precipitation at all stations. Table 1 and Table 2 demonstrate how much better the downscaled GCM precipitation matches the observations than do the raw GCM values. In addition, these tables show that the downscaling reduces some of the uncertainty in the GCM projections (there is less variability across models with the downscaled data than with the raw GCM data).

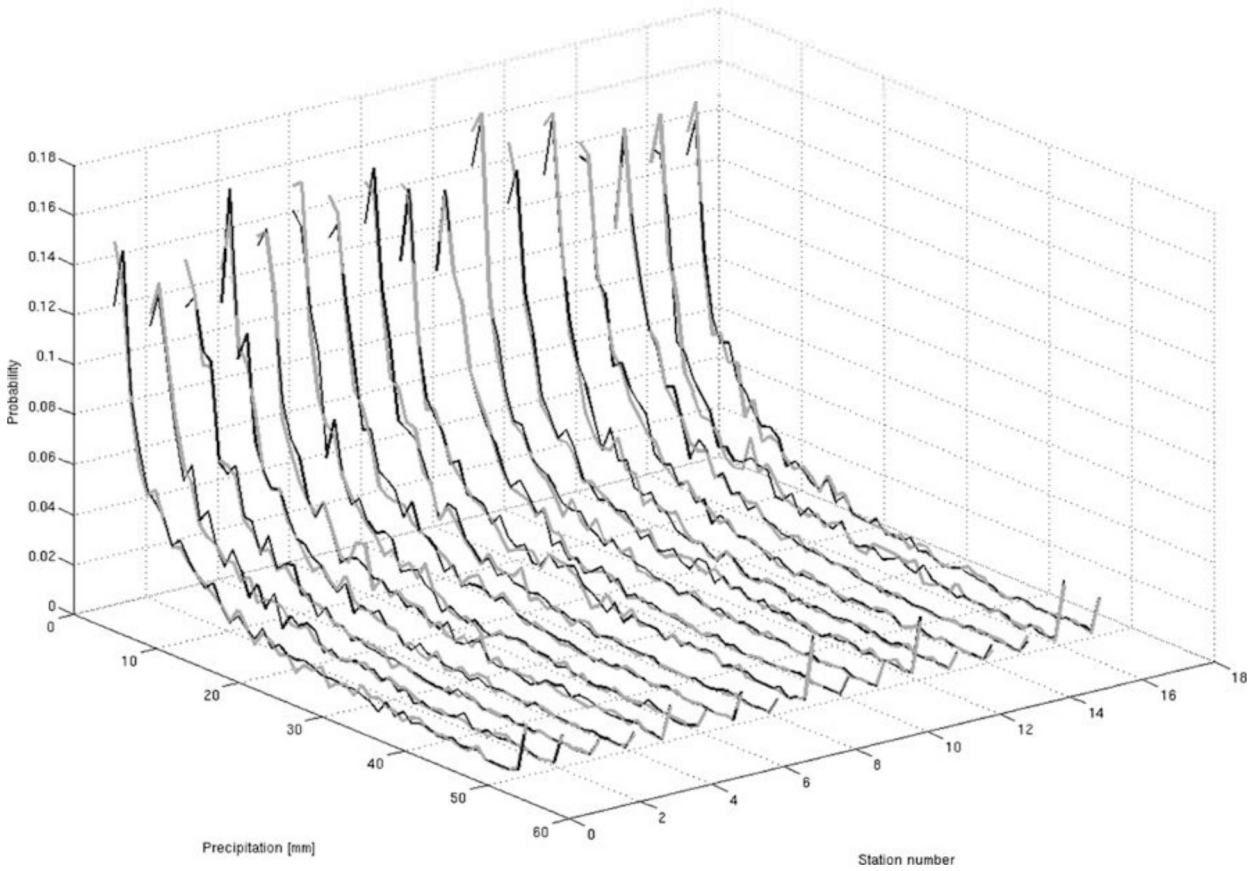

Figure 1. Probability distributions of observed (black) and downscaled (gray) daily precipitation over the 17 stations during the period 1079-2005. (From Ning et al., 2012a)

Table 1: Percent absolute errors of downscaled and raw GCM precipitation with respect to Observations, averaged across the 17 stations and for all months from 1961-2000. (Modified from Ning et al., 2012a)

Model	Downscaled Average Monthly Precipitation	Raw Average Monthly Precipitation	Downscaled Average Monthly Number of Rain Days	Raw Average Monthly Number of Rain Days
CGCM 3.1	2.1	10.5	3.3	101.5
CNRM-CM3	9.4	13.1	5.9	97.4
CSIRO Mk3.0	2.7	18.3	5.6	65.8
GFDL CM2.0	7.0	9.1	5.6	77.6
GISS-ER	19.4	45.0	12.0	47.1
IPSL CM4	5.2	25.1	4.2	79.4
MIUBECHOG	7.7	9.8	3.8	107.3
MPI ECHAM5	3.4	11.5	3.7	42.0
MRI CGCM 2.3.2a	6.7	24.8	5.1	41.7
Mean	7.1	18.6	5.5	73.3

Table 2: Percent absolute errors of downscaled and raw GCM precipitation with respect to Observations, averaged across the 9 GCMs and for all months from 1961-2000 (Modified from Ning et al., 2012a)

Station	Downscaled Average Monthly Precipitation	Raw Average Monthly Precipitation	Downscaled Average Monthly Number of Rain Days	Raw Average Monthly Number of Rain Days
Allentown	7.6	17.4	4.6	83.2
Chambersburg	7.5	19.2	4.9	99.0
Franklin	5.5	17.3	7.4	68.1
Greenville	5.1	17.5	2.5	65.0
Harrisburg	4.7	16.8	4.6	83.7
Johnstown	5.0	16.8	8.4	47.6
Montrose	6.6	21.0	7.8	53.3
New Castle	4.1	19.7	3.0	73.5
Palmerton	8.0	18.9	2.8	101.9
Ridgway	4.6	16.7	2.4	55.6
State College	8.8	18.2	6.8	76.0
Stroudsburg	13.0	21.4	8.0	75.3
Towanda	6.9	25.2	5.3	93.7
Uniontown	8.0	18.4	7.3	63.3
Warren	4.4	19.6	2.1	45.5
West Chester	11.5	16.4	7.1	79.5
York	9.0	15.5	7.9	81.9
Mean	7.1	18.6	5.5	73.3

The projected change in rainfall distributions over Pennsylvania are shown in Figure 2. The columns are annual, summer and winter anomalies; the top row is the downscaled rainfall and the bottom row is the raw GCM projections. It is apparent from the diagram that the GCM data over-estimate the changes and there are significant differences in spatial distributions, particularly annually and in winter. The figure shows differences in mm/month and the data are averaged across all GCMs. There are, however, large differences between models The projected change in rainfall for one station (Harrisburg) is shown in Table 3. The raw GCM projections show changes between -8.0 mm to ~25 mm per month while the downscaled range is 0.6 mm to 8.7 mm. Again, there is more consistency between models with the downscaled precipitation changes, with the downscaling generally projecting a smaller increase than the raw GCMs

Table 3: Change in Downscaled and Raw GCM projections of Precipitation for one station (Harrisburg) Future (2046-65) minus Present (1961-2000). Modified from Ning et al., 2012b)				
Model	Change in Downscaled Average Monthly Precipitation (mm)	Change in Raw Average Monthly Precipitation (mm)	Change in Downscaled Average Monthly Number of Rain Days	Change in Raw Average Monthly Number of Rain Days
CGCM 3.1	8.7	8.7	0.4	-0.2
CNRM-CM3	6.1	10.0	0.2	0.7
CSIRO Mk3.0	2.0	5.7	-0.1	-0.2
GFDL CM2.0	2.3	13.2	0.5	-0.2
GISS-ER	3.1	24.7	0.4	3.26
IPSL CM4	6.6	-7.5	0.0	-1.6
MIUBECHOG	0.6	-8.0	-0.1	-1.4
MPI ECHAM5	6.4	8.1	0.5	0.1
MRI CGCM 2.3.2a	0.8	3.6	-0.3	-0.5
Mean	3.1	6.5	0.2	0.0

2.2 Trading Space for Time in Streamflow Prediction Under Climate Change

A standard approach for estimating streamflow under changing climate conditions is to take a hydrologic model developed for current conditions using historic data and force the model with estimates of future climate change. However, there is a concern that the parameterization of the is biased toward the climate used to train the model, and that this will negatively impact the quality of the future change projections. This issue was addressed in the present study by adopting a framework used to estimate model parameters for ungauged river basins.

In this case, we regionalize the climate-dependent streamflow characteristics using 394 U.S. watersheds. The methodology then assumes that this spatial relationship between streamflow and climate is similar to what we would see at a single location as climate changes. By using these observed streamflow-climate relationships across the country and applying them to a single location as climate changes, we are, in effect, trading space for time in the derivation of the climate-dependent streamflow parameters in the model. The method proceeds by developing a model for the current climate at a location, projecting ahead the likely climate change, modifying the climate-dependent parameterizations in the model by extrapolation from basins currently under those climate conditions, and then rerunning the model for the future climate. This recalibration of the model for the new climate is conducted within a Bayesian framework to produce ensemble predictions of continuous streamflow. The trading-space-for-time approach is illustrated in (Figure 3).

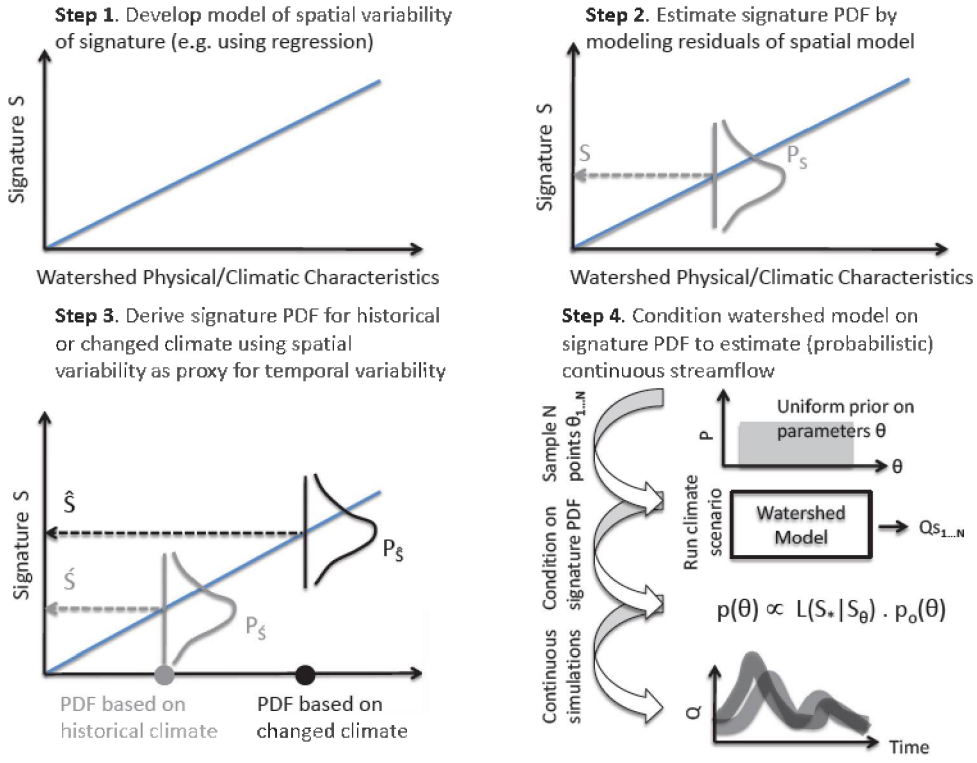

Figure 3. Deriving Probability Distributions of Streamflow for Climate Scenarios. In step 4, ϑ represents the model parameters, $Qs_{1....N}$ represents the model simulations, S_* is the expected value of the signature derived from the regionalized relationship and S_θ is the value of the signature for the parameter θ. (from Singh et al., 2011)

The method was tested using five U.S. watersheds in different climate regimes. The watersheds are described in Table 4 and Figure 4. Fifty years of data from the 394 watersheds were used in regression analysis to develop relationships for the climate-related streamflow characteristics. These were then evaluated against the five selected watersheds.

Table 4: Validation Watersheds for the Base Period 1958-1968 (Singh et al., 2011)

Watershed State	Lochsa Idaho/Montana	Lower Androscoggin Maine/New Hampshire	Escambia Alabama/Florida	Meramec Missouri	Yampa Colorado
USGS ID	13337000	1055500	2375500	7019000	9251000
Size [km^2]	3051	438	9886	9811	8832
Mean Elevation [m]	1584	190	95	279	2364
Climate Regime	Energy Limited	Energy Limited	Even	Slightly Water Ltd	Water Limited
Aridity Index	0.64	0.86	1.04	1.37	1.81
Precip. as Snow [%]	56.0	29.5	0.42	7.5	48.9
Mean Annual P [mm yr^{-1}]	1314	1018	1407	905	556
Mean Annual Q [mm yr^{-1}]	911	541	525	214	132
Mean Annual PE [mm yr^{-1}]	841	878	1464	1238	1007
Monthly NSE*	0.93	0.87	0.85	0.81	0.80
* Nash Sutcliffe Efficiency for Base Period (1958-1968)					

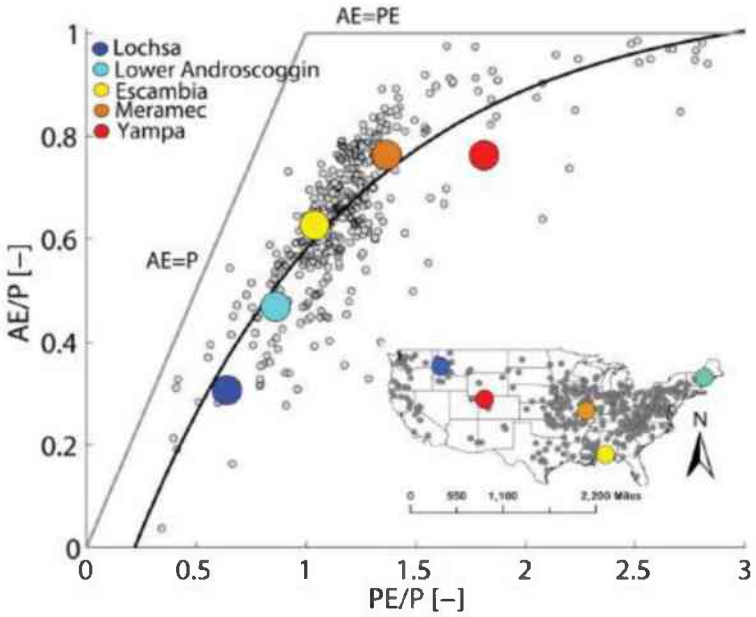

Figure 4: The Budyko Curve for the 394 watersheds (grey dots). The five study watersheds are highlighted and the black curve is a fitted Schreiber model. AE, PE and P are the long-term actual evapotranspiration, potential evapotranspiration, and Precipitation respectively. AE/P is equal to 1 – runoff ratio, and PE/P is the aridity index. (from Singh et. Al., 2011)

Figure 5 shows the validation of the methodology – plotting the ratio of the validation period stream flow to the base streamflow for five validation periods for each of the five basins. The most probable flow for Type H and for Type C refers to flow with model parameters based on the historic record and for flow based on model parameters adjusted for changing climate, respectively. Figure 5 shows that Type C predictions are closer to th4e observed values as the percentage change in streamflow increases. From these data, it appears that historical calibration will be better if the climate change is small, but that the changed parameters will improve performance as the degree of climate change increases.

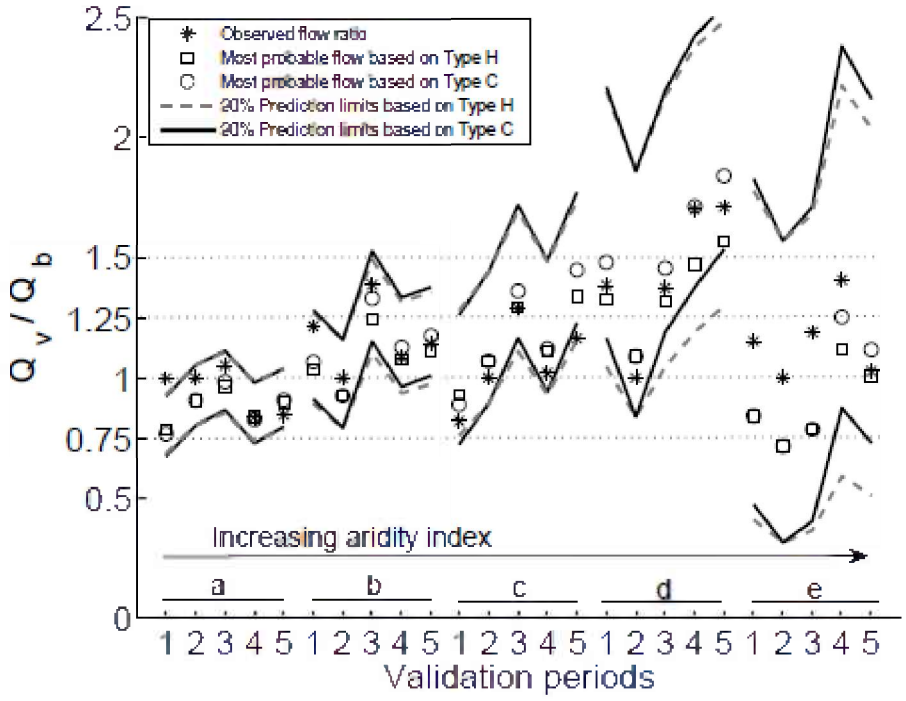

Figure 5: Validation Plot Showing the Ratio of Validation Period Streamflow (Qv) to Base Period Streamflow (Qb) for the Five Study Wartersheds. Watersheds are sorted by increasing aridity index [(a) Lochsa, (b) Lower Androscoggin, (c) Escambia, (d) Meramec, (e) Yampa]. Validation periods are 1: 1948-58, 2; 1958-68, 3:1968-78, 4: 1978-88, 5: 1988-96. Dashed and continuous lines show the 90% prediction limits for historical conditioning and conditioning based on changing climate respectively.

These five watersheds were then tested with synthetic climate scenarios generated by increasing mean temperatures up to 8°C and changing mean precipitation between -30% and +40% of their historic conditions. The results indicated that, for the most part, watersheds were more sensitive to rainfall than temperature and that Type C projections are more sensitive to changes in climate. The further the future scenarios depart from the historical period, the greater is the difference between the two projections. Also significant is that the Type H projections are a linear function of the change in climate, whereas increasingly non-linear responses are seen in the Type C projections as watersheds get drier.

2.3 A Vulnerability Approach to Identifying Adverse Climate and Land Use Change Combinations

The climate downscaling provides more reliable information at the regional scale and, to some degree, reduces the uncertainty in precipitation projections obtained from the suite of GCMs used. By employing a trading-space-for-time approach to parameterizing streamflow models, we also produce models that may be more representative of local conditions under climate change. However, there is still considerable uncertainty transferred through the model hierarchy. This uncertainty makes the streamflow projections more problematic for water managers and decision makers. To address this issue, we take a bottom up approach that first establishes the vulnerabilities in the system, and then looks to see what degree of climate and land use change is necessary to exceed those levels, and then

interrogates the climate downscaling data to determine how likely it is that the watershed will experience that degree of change.

The approach uses Classification and Regression Trees (CART) to establish the combinations of climate and land use change that lead to vulnerability, and those that do not. We begin with a feasible space of climate and land use changes. In this case, land use is represented in the analysis as the fraction of deep-rooted vegetation in the watershed. In an operational application, we would then ask the relevant stakeholders to provide their definition of vulnerable ranges of streamflow indicators. In this case we apply the method to a Pennsylvania watershed using nine ecological and water resources related streamflow indicators and group the results into one of seven categories depending on the number of standard deviations the indicator is away from the historical mean :

- Class 1 – Historical range: $\mu-2\sigma < Value < \mu+2\sigma$
- Class 2 – Slightly higher than historical range $\mu+4\sigma < Value < \mu+8\sigma$
- Class 3 – Much higher than historical range $\mu+8\sigma < Value < \mu+12\sigma$
- Class 4 - Slightly lower than historical range $\mu-4\sigma > Value > \mu-8\sigma$
- Class 5 – Much lower than historical range $\mu-8\sigma > Value > \mu-12\sigma$
- Class 6 – Extremely high ranges $\mu+12\sigma < Value$
- Class 7 – Extremely low ranges $Value < \mu-12\sigma$

The following description of the CART methodology and the hydrologic model used is extracted from Singh et al. (2014). Using *N* climates and *P* parameter combinations, we derive *N*x*P* values of hydrologic indicators of interest by driving the hydrologic model with these combinations and assign them to their specific class. Next, we use the classification and regression tree (CART) to relate the climate and land use changes to the different classes of the streamflow indicator. CART is a binary recursive partitioning algorithm that divides the input space of multiple variables into sub-spaces, with each sub space related to a particular class of output variable [*Breiman et al.*, 1984]. At each stage, the tree partitions the space based on maximum gain in information. Thus, through CART analysis, we can assess the critical changes in land use and climate required to push the streamflow indicators into different regimes (represented by the indicator classes).

The hydrologic model structure used in this study is adapted from the top-down modeling framework by *Bai et al.*, [2009] and *Farmer et al.* [2003]. The model has a lumped parsimonious model structure, with daily resolution of inputs and output streamflow. The model comprises of a snow module followed by a soil moisture accounting module and a routing module. There is possibility for recharge from the saturated soil store to the deeper groundwater store. The soil moisture accounting module splits the soil into two layers – unsaturated and saturated stores. The soil depth is modeled using a multiple bucket scheme based on the ten-bucket Xinanjiang-model distribution [*Zhao et al.*, 1980; *Son and Sivapalan*, 2007; *Bai et al.*, 2009]. The multiple buckets are filled and spilled in a parallel configuration. Evapotranspiration is estimated by dividing the catchment surface into bare soil and deep-rooted vegetation covered areas. The soil profile is divided into unsaturated and saturated zone. ET from saturated zone is proportional to the potential evaporation and soil moisture content. The saturated

zone evaporation is modeled similarly for both bare soil and vegetation covered fractions. The main difference in ET arises in the unsaturated soil store. In the unsaturated zone, the fraction of watershed covered by bare soils evaporates at a rate that is proportional to the soil water content and to the potential evaporation. In the case of vegetation-covered soils, transpiration from the unsaturated stores is controlled by field capacity parameter, if the soil moisture content is greater than field capacity, transpiration occurs at potential rate. The basic formulation is adapted from *Bai et al.* [2009], with modifications for including phenology and leaf area index from *Sawicz et al.* [2013]. The growing behavior of vegetation, efficiency of water extraction from the soil, and variable canopy interception are included in the model to represent phenology in three ways. Above 10°C, water extraction by vegetation is considered unimpeded and is set at its maximum capacity. Below -5°C, water extraction efficiency is considered to have stopped so there is no evapotranspiration. Between these two ranges, a linear relationship between extraction efficiency and temperature is assumed. The canopy interception is modeled as maximum canopy interception during summer months and a minimum during winter months. A sinusoidal function is used to describe the canopy interception for periods between summer and winter.

The approach is tested on the Lower Juniata at Newport PA (Figure 6). 10000 random parameter sets

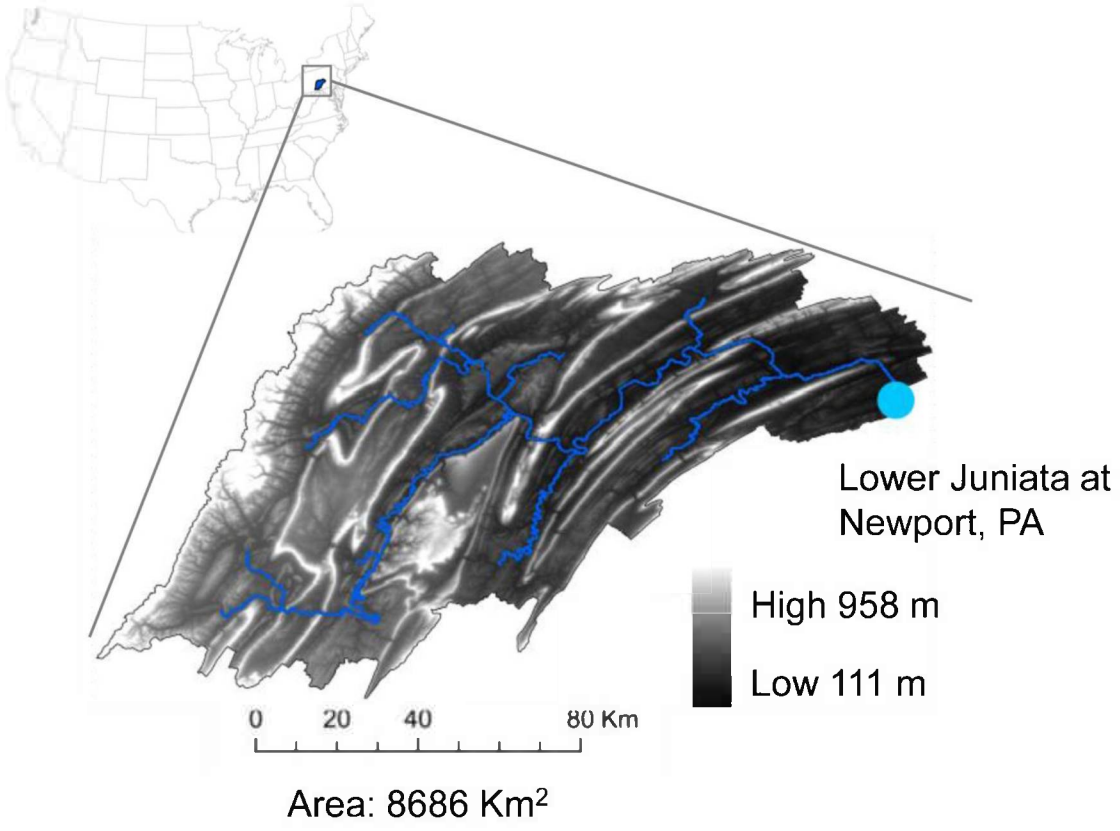

Figure 6: The Study Area on the Lower Juniata in Pennsylvania (Singh et al., 2014). The streamflow guage is located at Newport, PA.

are generated from a-priori ranges for the nine indicator parameters described in Table 5. 1948-1958 is

used as the climatological base period and climate change scenarios are generated from -50% to +505 precipitation change (in 10% steps) and for temperature changes of 0°C – 8°C in 1 degree steps. The hydrologic model is, therefore, driven with 10,000 parameter combinations and 99 climates, resulting in 990,000 values for each of the streamflow indicators for use in the CART analysis. As one example, Figure 7 shows the resulting classification tree for flood frequency with fixed land use but changing climate. Each node in the tree is a logical expression. If the expression is true we follow the left branch, if not true we follow the right. In this manner we eventually reach a terminal node (leaf) showing the indicator class that

Table 5: Definition of the Hydrologic Indicators Used in the Study (based on Olden and Poff, 2003).

Hydrologic Indicator	Category	Definition	Units
Mean annual runoff	Magnitude	Mean annual flow (normalized by catchment area)	mm/year
Minimum April flow	Magnitude- high	Mean minimum monthly flow for April across time period of study	mm/day
Maximum August flow	Magnitude-low	Mean maximum monthly flow for August across time period of study	mm/day
Low flow pulse count	Frequency – low	Number of annual occurrences during which the magnitude of flow remains below a lower threshold. Hydrologic pulses are defined as those periods within a year in which the flow drops below 25th percentile of all daily values for the time period	[-]
Flood frequency	Frequency – high	Same as above where high pulse is defined as 3 times the median daily flow	[-]
Low flow pulse duration	Duration – low	Mean duration of low flow pulses defined above	[days]
High flow pulse duration	Duration – high	Mean duration of high flow pulses with high flow cutoff at 75th percentile of the daily flows of the entire record	[days]
Seasonal predictability of non-flooding	Timing of change	Maximum proportion the year (number of days/365) during which no floods have ever occurred over the period of record. Floods are defined as flow values greater than or equal to flows with 60% exceedance probability (1.67 year return interval)	[-]
Reversals	Rate of change	Number of negative and positive changes in water conditions from one day to the next	[-]

results from the combination of different logical expressions. In this case, the primary control for this indicator is precipitation, shown as the ratio of mean annual precipitation in the future to that of the present (Pratio), followed by the recession coefficient (Ass) that describes the recession from the

subsurface soil moisture source. The third control is the maximum height of soil moisture storage (Sb). This indicates that the frequency of high floods depends first on the watershed climate, followed by its ability to release water from the subsurface and the amount of water that can be stored in the subsurface. The diagram also shows the probabilities associated with the seven classes. Figure 7b also denotes the different pathways that lead to vulnerability of the indicator by solid black lines. Following the left branch of the classification tree, we find that if mean annual precipitation changes remain within -5% to 15% of the historical value, the most likely values of flood frequency are Class 1, i.e., the indicator remains within historical variability. On the other hand as precipitation rises beyond 15% of its historical value, model parameters emerge as significant controls on the classes for the indicator. If precipitation increases, both the amount of increase and other watershed properties will govern the future values for flood frequency. On the other hand, if precipitation decreases, precipitation itself will be the dominating control on this indicator.

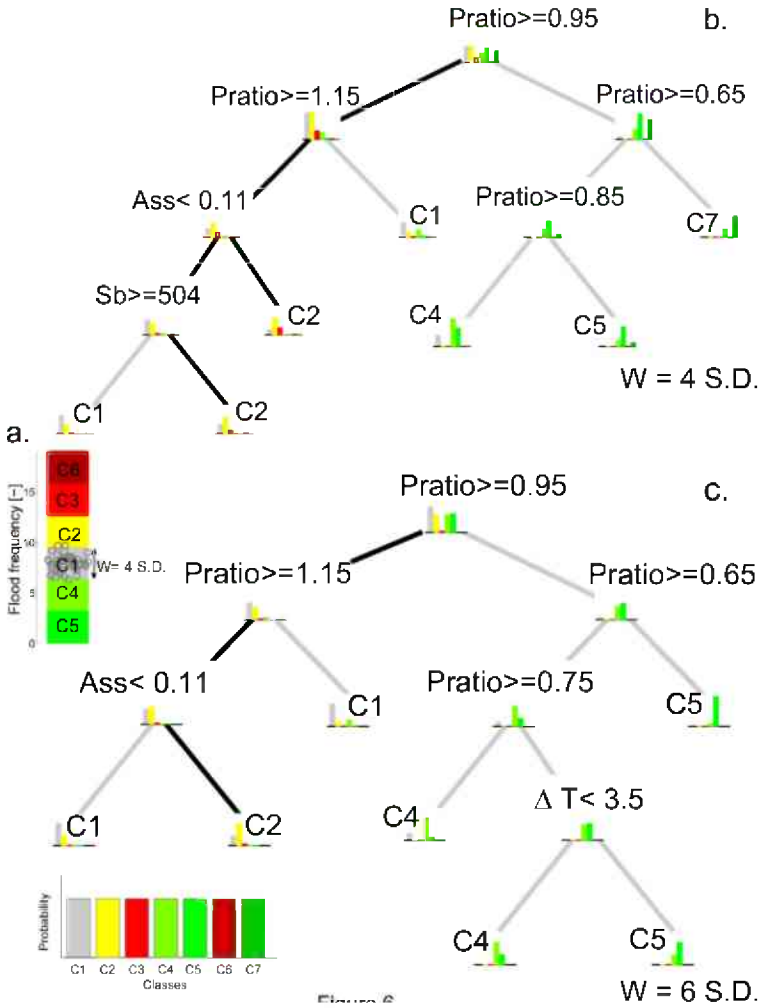

Figure 7: Class Assignments for Flood Frequency Indicator for class widths of 4σ (b) and 6σ (c).

Figure 8 shows one example for how this approach compares to more traditional top-down modeling where (a) shows the projected downscaled future precipitation and temperature from the nine different GCMs. (c) shows the projected runoff based on a hydrologic model driven by the downscaled climate

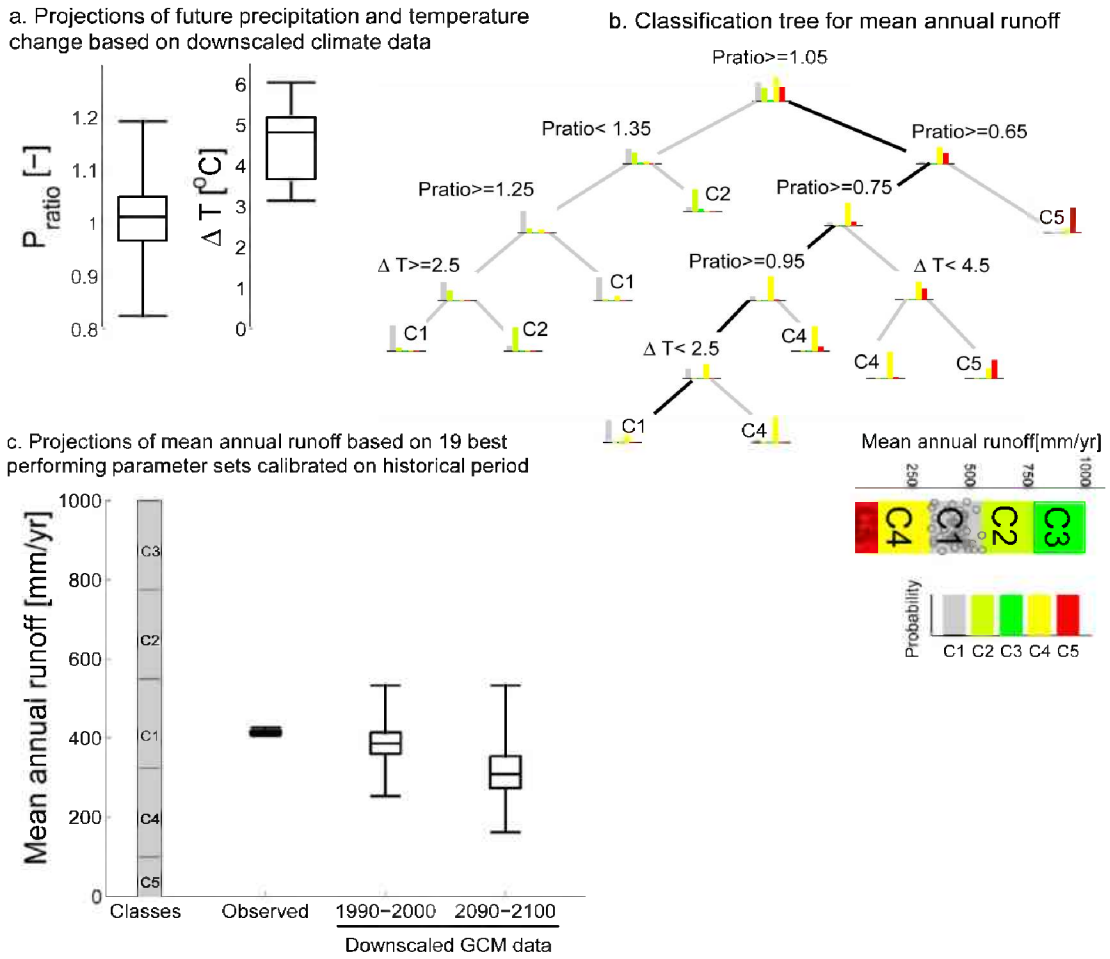

Figure 8: Comparison with Downscaled Climate Change Projections. (a) shows the downscaled projections with Pratio expressed as the ratio of mean annual precipitation for (2090-2100) projections to mean annual rainfall for 1990-2000 and ΔT is the difference in mean annual temperatures between the same time periods. (b) is the classification tree for mean annual runoff with the heavy black lines representing streamflow obtained by navigating the tree using the downscaled projections from (a). (c) shows the streamflow projections obtained from a traditional top down approach, driving the hydrologic model from the downscaled climate data with the model parameters fixed at their historically calibrated values.

data, and where the ranges reflect the variability in the downscaled projections and the uncertainty in the hydrologic model. (b) shows a CART decision tree generated through the 990,000 realizations of the hydrologic model driven by the range of climate and land use change scenarios and for a range of hydrologic parameterizations. Again, the bar graphs at the end of each pathway show probabilities of the parameter (i.e. mean annual runoff) ending in one of five vulnerability classes. C1 is similar to

present, while C2/C3 and C4/C5 are increasingly vulnerable (wetter and drier, respectively). The dark black line shows the pathway followed based on the climate downscaling. The analysis indicates that while there are lots of pathways to vulnerability, none are likely given the projected climate change. The conclusions from the CART analysis are potentially much more useful to a decision maker than is the wide range in potential future streamflows derived from the more traditional top-down, hierarchical modeling approach.

References:

Bai, Y., T. Wagener, and P. Reed (2009), A top-down framework for watershed model evaluation and selection under uncertainty, *Environ. Modell. Softw.*, doi:10.1016/j.envsoft.2008.12.012.

Breiman, L., J.H. Friedman, R.A. Olshen, and C.J. Stone (1984), Classification and regression trees, CRC Press.

Farmer, D., M. Sivapalan, and C. Jothityangkoon (2003), Climate, soil, and vegetation controls upon the variability of water balance in temperate and semiarid landscapes: Downward approach to water balance analysis, *Water Resour. Res.*, 39(2), 1035.

Son, K., and M. Sivapalan (2007), Improving model structure and reducing parameter uncertainty in conceptual water balance models through the use of auxiliary data, *Water Resour. Res.*, 43, W01415, doi:10.1029/2006WR005032.

Zhao, R.J., Y.L. Zhang, L.R. Fang, X.R. Liu, and Q.S. Zhang (1980), The Xinanjiang model, in, *Hydrological Forecasting*, IASH Publ., 129, 351-356.

3. Publications Supported in Whole or in Part Under This Project:

Refereed Publications:

Ning, L., M. E. Mann, R. G. Crane, T. Wagener, R. Najjar, R. Singh. Probabilistic Projections of Anthropogenic Climate Impacts on Precipitation for the Mid-Atlantic Region of the United States. **J. Climate**, 25:5273-5291 (2012).

Ning, L., M. E. Mann, R. G. Crane, T. Wagener. Probabilistic Projections of Climate Change for the Mid-Atlantic Region of the United States—Validation of Precipitation Downscaling During the Historical Era. **J. Climate**, 25:509-526 (2012).

Singh, R., T. Wagener, R. Crane, M.E. Mann, L. Ning. A vulnerability driven approach to identify adverse climate and land use change combinations for critical hydrologic indicator thresholds—Application to a watershed in Pennsylvania, USA**. Water Resources Research**, DOI: 10.1002/2013WR014988 (2014)

Singh,R., K. van Werkhoven, T. Wagener. Hydrological impacts of climate change in gauged and ungauged watersheds of the Olifants basin: a trading-space-for-time approach**, Hydrological Sciences Journal**, 59:1, 29-55, DOI: 10.1080/02626667.2013.819431 (2014)

Singh, R., T. Wagener, K. van Werkhoven, M. E. Mann, and R. Crane. A trading-space-for-time approach to probabilistic continuous streamflow predictions in a changing climate – accounting for changing watershed behavior. **Hydrol. Earth Syst. Sci**., 15:3591–3603 (2011).

Doctoral Theses:

Probabilistic Estimation and Validation of Regional Climate Change Using Statistical Downscaling Methods. The Pennsylvania State University (2012).

Singh, R. An Uncertainty Framework for Hydrologic Projections in Gauged and Ungauged Basins Under Non-Stationary Climate Conditions. The Pennsylvania State University (2013).